RILEM Technical Letters (2025) 10: 1-14
https://doi.org/10.21809/rilemtechlett.2025.214

Thermodynamic modeling: Success in cement science – Untapped potential in corrosion research

Fabio E. Furcas[1,2,*], Barbara Lothenbach[2], Shishir Mundra[1], O. Burkan Isgor[3], Mette R. Geiker[4], Ueli M. Angst[1]

[1]Institute for Building Materials, ETH Zürich, Switzerland
[2]Empa, Concrete & Asphalt Laboratory, Switzerland
[3]School of Civil and Construction Engineering, Oregon State University, United States
[4]Department of Structural Engineering, Norwegian University of Science and Technology, Norway

Received: 27 January 2025 / Accepted: 01 April 2025 / Published online: 08 April 2025

Abstract

For more than a century, the corrosion of steel in concrete has prevailed as a complex and yet poorly understood phenomenon, with many durability design approaches relying on phenomenological or semi-empirical service life models. The increasing societal demand to maintain aging infrastructure, the development of new cementitious binders and the push towards an environmentally more benign and circular concrete economy exacerbate the need for a more comprehensive scientific understanding of the underlying physicochemical processes, particularly in the absence of long-term empirical data. This manuscript retraces the history of thermodynamic modeling in cement and concrete research, examining early concepts, the barriers to adoption, and the pivotal role of modern Gibbs free energy minimisation solvers towards its broad level of acceptance within the scientific community. We further examine the current use of thermodynamic modeling techniques in corrosion science, emphasizing the limitations of classical potential-pH stability diagrams and addressing the widespread misconception that thermodynamics and kinetics are opposing concepts. Finally, we explore the opportunity to leverage the recent developments in the field of cement science and adopt thermodynamic modeling techniques in corrosion research, thereby addressing open questions related to the corrosion of steel in concrete.

Keywords: Corrosion; Steel; Concrete; pH; Durability.

1 Introduction

The corrosion of steel reinforcement in concrete remains a multifaceted and not yet comprehensively understood phenomenon. Existing predictive approaches typically describe the behavior of reinforced concrete structures through a combination of empirical relations and simplified representations of the underlying physicochemical processes [1-3]. Some of these predictive approaches may, under some conditions, support decision making in engineering, especially when calibrated against practical long-term experience. However, since such phenomenological approaches lack a detailed understanding of the fundamental processes at play, their applicability to modern materials, with no empirical track records, is associated with large uncertainties.

The motivation to advance our understanding of steel corrosion in concrete is fundamentally driven by societal needs. In addition to the environmental burden, safety considerations and traffic jams, addressing infrastructure corrosion demands substantial financial resources [4, 5]. Given that the civil engineering sector is undergoing large transitions towards more sustainable construction practices [6-10], it becomes increasingly difficult to justify the application of empirical models to ensure the long-term durability. An integral part of this transition is the development of new construction technologies such as 3D printing and digital fabrication [11, 12], as well as low-carbon binders [13], featuring a chemical environment inherently different from those seen in traditional Portland cement-based systems. These developments present a significant challenge in predicting the long-term performance of civil infrastructure, underlining the necessity for fundamental science-based approaches to predict the corrosion of steel in concrete [14].

Over the course of the past decades, advancements in analytical and computational methods have opened new avenues for exploring the interactions of steel reinforcement

*Corresponding author: Fabio E. Furcas, E-mail: ffurcas@ethz.ch

with the surrounding concrete matrix at multiple scales [15-17]. High-resolution chemical imaging techniques including X-ray computed tomography (XCT) and X-ray absorption spectroscopy (XAS) allow for detailed observations of the presence of water in micropores of cementitious materials [18] and the morphology and composition of corrosion products at the metal-electrolyte interface [19, 20].

Nanoscale surface characterization techniques such as FIB/TEM [21], electron energy loss spectroscopy (EELS) [22] and X-ray photoelectron spectroscopy (XPS) [23, 24] have helped develop fundamental understanding of passivity and chloride-induced depassivation of steel in alkaline environments. Simultaneously, computational modeling approaches enable simulations of the electrochemical processes that govern corrosion kinetics at the atomistic scale [25, 26] and corrosion-driven damage in porous media [27]. Among the various computational approaches, thermodynamic modeling has emerged as a particularly powerful tool for advancing our understanding of the chemistry of cements [28, 29]. Thermodynamic models predict the phase equilibria and the stability of various aqueous, solid or gaseous phases within the cementitious matrix. Coupled with transport solvers [30, 31], they can further compute the spatial distribution of dissolved species such as chlorides, carbonates and sulfates, all of which play a crucial role in the initiation and propagation of reinforcement corrosion. Alongside with the development of thermodynamic databases, these modeling approaches have become an indispensable tool to investigate the chemical alteration of cement-based materials, advancing our understanding of cement hydration [32-34], phase equilibria [35] and its microstructural evolution [36, 37]. Thermodynamic modeling has also become a necessary tool in the efforts to understand the effects of low-carbon binder systems on reinforcement corrosion as these binders can alter the pH buffer capacity of the cementitious systems and affect the cation and anion balance in the pore solution [38-40].

Despite these advancements, our understanding of the corrosion of steel in concrete has largely remained empirical, particularly with regard to the prediction of corrosion initiation and propagation of corrosion-driven damage [41]. One of the contributing factors to our limited understanding is that existing modeling approaches are highly simplified. For instance, all existing models for concrete structures exposed to chloride environments rely on the concept of critical chloride threshold, a sharply defined trigger for corrosion, followed by a period of active corrosion. It has been shown in a recent paper [2] that this simplification, despite its practical benefits, has been detrimental in developing science-based predictive models. This is because the narrow focus on the concept of the critical chloride threshold has impeded the development of alternative modeling approaches to describe the processes related to corrosion initiation. Moreover, regarding later stages beyond corrosion initiation, numerous models have been developed with a primary focus on mechanical aspects, such as volume expansion of corrosion products and the resulting cracking of concrete, often by scholars with a background in mechanical modeling. Unfortunately, these models often fail to fully account for the chemical and electrochemical aspects of the underlying processes, a simplification that has been identified as a reason for the generally poor predictive power of such models [16].

Another example of oversimplifying corrosion lies in the assessment of the electrochemical stability of steel in concrete, which is often based on the Pourbaix diagram of iron in pure water. The set of chemical species that constitute the electrochemical passivity and corrosion regime of iron appear to be selected based on tradition, instead of scientific merit or experimental evidence. One of the major pitfalls associated with this approach is that the electrochemical stability diagram is rarely tailored to the actual exposure conditions and the resulting chemical environment at the steel-concrete interface: For instance, whilst it is well established that the presence of chlorides and carbonates can accelerate the rate of reinforcement corrosion, both the formation of iron-carbonate and iron-chloride complexes are commonly not considered in Pourbaix diagrams. In addition to these methodology-inherent limitations, Pourbaix diagrams, and thermodynamic modeling approaches in general, do not contain any information about the rate of corrosion, which is determined by the transient physicochemical conditions at the metal-electrolyte interface. Consequently, thermodynamic and kinetic modeling approaches are sometimes regarded as mutually exclusive. The authors of this document have, during scientific discussions in the field of corrosion science, witnessed that thermodynamic considerations are sometimes undervalued or deemed less effective compared to kinetic considerations. While obviously both concepts – thermodynamics and kinetics – have their limitations, it is the authors' opinion that some of the open questions that have prevailed within the academic community for several decades can, in fact, be addressed, utilizing the very thermodynamic modeling approaches that have already been adapted widely and successfully in the field of cement and concrete research.

This manuscript focuses on the evolution of thermodynamic modeling as a valuable tool in cement and concrete science over the past decades and its promising use for prediction of corrosion behavior of reinforcement. We first review the historical development of thermodynamic modeling approaches, with a particular focus on the challenges overcome towards their broad level of acceptance in cement science today. We proceed to investigate the adoption of thermodynamic modeling techniques in corrosion science. Retracing the development of electrochemical stability diagrams and their widespread use in corrosion education, we explore the actual and perceived limitations of thermodynamic modeling techniques to predict the corrosion of steel in concrete. Under consideration of recent advancements in material characterization, microscopy and other computational techniques, we demonstrate how the existing gaps in our phenomenological understanding can be bridged. Analogous to their establishment in the field of cement and concrete research, we seek to develop a set of key milestones that need to be reached to leverage the full

potential of thermodynamic modeling techniques, ultimately contributing to more reliable predictions of the corrosion behavior of reinforced concrete structures and the electrochemical degradation of metals in general.

2 Review of thermodynamic modelling for cement

Thermodynamics are essential to our understanding of chemical reactions within hydrated cements and their interaction with steel bars. Thermodynamic models can reliably predict the composition of hydrated cements, their chemical compositions [35, 42] as well as their potential interactions with the service environment [43, 44]. Many studies have shown that such thermodynamic modeling predictions are reliable and accurate, if complete, internally consistent and accurate thermodynamic databases are used.

The first rather complete compilation of thermodynamic data for hydrated cements was published as early as 1965 by Babushkin et al. [45]. In the following years, several additions or partial databases were published, focusing on the solubility of cement hydrates based on the latest experimental data available at that time [32, 46-51]. The two excellent datasets published in 1992 by Reardon [52] and by Bennet et al. [53] represented a first major update, followed by the Cemdata07 database [36, 54-57] published in 2006 and the Thermoddem cement database published in 2010 by Blanc et al. [58, 59]. The Cemdata database experienced a major update in 2019 [42].

Since the 1960's research in thermodynamics applied to hydrated cements has gradually sped up and became an important tool in the last decades. As schematically illustrated in Figure 1, the number of scientific publications registered on the Scopus database under the key words "thermodynamic modeling AND cement" exceeds a total 5000 in the years from 1991 to 2024, with many articles being published in the wake of the most recent database updates in 2006, 2010 and 2019. Publications yielding search results for the keywords "thermodynamic modeling AND cement AND corrosion" remain comparatively scarce.

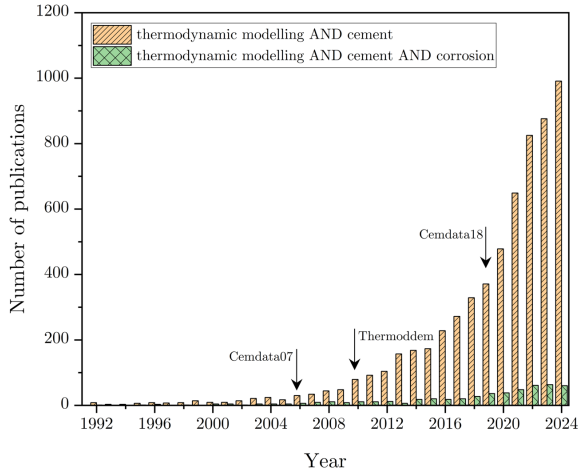

Figure 1. Number of scientific publications registered on the Scopus database from 1991 to 2024, as determined by Boolean search for the set of key words "thermodynamic modeling AND cement" and "thermodynamic modeling AND cement AND corrosion". In comparison to the abundance of scientific literature concerned with thermodynamic modeling of cement, a small number of articles yield search hits for the latter key words. It is emphasized that the registered number of publications for the first set of key words experiences an incline in the years subsequent to the release of Cemdata07 in 2006, Thermoddem in 2010 and the Cemdata18 database in 2019.

Three main factors contributed to the increased use of thermodynamic modeling to predict the composition of hydrated cements. They are discussed in Subsections 2.1 to 2.3.

2.1 Development of comprehensive thermodynamic databases

The development of reliable and relatively comprehensive thermodynamic databases for hydrated cements, e.g., [42, 58, 59], has been fundamental for making accurate thermodynamic predictions. Such databases are generally developed based on meticulous measurements of the solubility of well characterised phases in under- and oversaturation experiments at different temperatures [60-63], combined with careful observation for newly formed phases during equilibration. In some cases, solubility measurements were also combined with the fitting of missing, unknown thermodynamic properties versus known fields of stability, as e.g., done for databases for hydrothermal systems [58, 64]. The rigorous validation of thermodynamic modeling techniques has resulted in successively better matches between model predictions and experimental observations. This demonstrated utility has, in turn, fostered growing confidence within the scientific community.

2.2 Advancements in computational tools

Another key factor that contributes to the broad adoption of thermodynamic modeling techniques is the development and availability of well tested computational tools, such as the geochemical modeling package PHREEQC [65] or the GEM-Selektor code [66, 67]. The Reaktoro framework [68] offers further integration with on-demand machine learning (ODML) to accelerate chemical reaction calculations. Other tools including the electrochemical modeling package PourPy [69] are designed to complement existing frameworks, providing calculation routines to construct particular types of thermodynamic stability diagrams, e.g., the stability of chemical elements and compounds as a function of the electrochemical potential and the pH. These computational tools can primarily be distinguished in terms of their calculation methodology, underlying databases and the scope of processes they can model. Amongst the calculation methodologies used to compute the equilibrium composition of the model system, computational tools generally revert to law of mass-action (LMA) approaches or minimize the Gibbs free energy of the system. LMA calculations, including reaction-path approach employed by the PHREEQC modelling package, require the explicit formulation of all reactions that can alter the chemical composition of the modeling system. Under the assumption that these reactions proceed equally rapid both in forward and backward direction, the corresponding equilibrium constant can be formulated as the

product of the activities (or concentrations) of all chemical species involved, raised to the power of their respective stoichiometric coefficients. In combination with a mass balance constraint, these LMA equations form a set of non-linear algebraic equations that can be solved iteratively. The LMA approaches are particularly efficient for systems with relatively few reactions that primarily involve the formation of aqueous species. Gibbs free energy minimization approaches, as implemented in GEMS and Reaktoro, on the other hand do not require the explicit formulation of all chemical reactions taking place. They use numerical optimization algorithms to minimize the total Gibbs free energy of the chemical system as a function of its composition and other thermodynamic state variables (e.g., pressure, temperature and volume). Though computationally more expensive that LMA approaches, they can handle complex multi-component, multi-phase and heterogeneous systems and are thus particularly suited to predict the chemical composition of hydrated cements. In addition to these methodology inherent differences, various modeling tools available vary in terms of their in-built activity coefficient models, their capability to perform temperature corrections, account for non-ideal interactions (e.g., solid-solution modelling), handle vapor-liquid interactions and their ability to simulate auxiliary multiphysics processes, such as mass transport. Table 1 summarizes the calculations methodology and modeling capabilities of selected computational tools discussed and used within this paper.

Although differing in user-friendliness, all geochemical modeling approaches will essentially give identical solutions using the same input data and same thermodynamic data sets. Both GEMS (2012) and PHREEQC (1995) and their respective general thermodynamic databases are freely available and relatively easy to use, which allows not only dedicated specialists, but also interested cement chemist and engineers to use thermodynamic modeling efficiently [70, 71]. In 2021, the development of the web application CemGems [72] has further facilitated the accessibility and ease of use of thermodynamic models. Based on the composition of the starting material, provided by the user, phase changes upon hydration or interactions with the environment can be obtained using predefined processes.

2.3 International collaboration

The success story in the field of cement and concrete research can, to some extent, also be attributed to ongoing international collaborations between modelers, experimentalists and users. Their joint efforts to disseminate knowledge within the scientific community beyond the publication of peer-reviewed research, e.g., through the organization of conferences and workshops, has played a crucial role in the widespread acceptance of thermodynamic modeling techniques to date.

2.4 Ongoing thermodynamic modelling work in cement and concrete research

The continuing effort of different groups to measure the solubility of additional hydrates and to generate missing thermodynamic data supported the rapid development and increased use of blended and alternative cement. Recent updates allowed to better predict the hydrates formed in alkali activated systems [73, 74], hydrated magnesium carbonates [75], magnesium phosphates [62, 76], magnesium silicates [77] and under hydrothermal conditions [64]. Also, updates in the description of alkali [78-80] and chloride binding by C-S-H [81, 82] as well as the potential formation of zeolites [83-85] is fundamental to predict the pH and the Cl/OH^- ratio in the pore solution of hydrated cements more precisely, one of the main factors affecting corrosion kinetics [86].

Although the available thermodynamic data allow to adequately describe most hydrated cement systems, new development and increased use of alternative cements lead to the necessity to measure and include data for additional hydrates such as hydrous carbonate-containing brucite (HCB) [75, 87], the binding phase in some magnesium carbonate cements, aluminum and iron-containing LDH phases [63, 88, 89], alkali silica reaction products [90, 91] or the alumina silica gel formed during carbonation of hydrated cements [92, 93], for which thermodynamic data are partially missing. Not only solid phases, but also the aqueous speciation greatly influences the hydrates formed; in particular reliable data for ternary silicon, iron(II) and iron(III) complexes or complexes with organic molecules at high pH values are missing or under debate [94-96].

One of the major problems in the application of thermodynamic models to cementitious systems is related to kinetic hindrance and the slow formation of some phases. Well known examples are quartz and crystalline calcium silicates, that form under hydrothermal but not at ambient conditions, although they are thermodynamically more stable than amorphous SiO_2 or C-S-H [58, 64, 87]. In the absence of additional kinetic treatment, thermodynamic modelling would thus predict the exclusive formation of the energetically more stable phases, rather than their experimentally observed amorphous or semi-crystalline counterparts. Siliceous hydrogarnet, which can incorporate aluminium and iron, is thermodynamically stable in hydrated Portland cements [97] and is expected to destabilise AFm phases in the long-term, but the formation of Al-rich siliceous hydrogarnet is slow, such that it can take several decades before AFm phases are replaced by Al-rich siliceous hydrogarnet [98]. The knowledge of dissolution and precipitation kinetics and their rate constants are fundamental for the prediction of transport within hydrated cements.

Table 1. Summary of the calculation methodology and additional modelling capabilities of selected thermodynamic modelling packages discussed and used within this paper.

Modeling package	Calculation methodology	Additional capabilities	Databases	Solid solution modelling	Electrochemical stability	Activity coefficient models	Temperature correction	VLE[3]
PHREEQC	LMA[1], reaction path	Transport	Pre-defined, user extensible	Basic (ideal behavior)	Redox-equilibria	Various, Debye-Hückel, Pitzer, SIT	Basic, in-built in database	Limited
GEMS	GEM[2]	Transport	Support for various, user extensible	Advanced (non-ideal), user-defined interaction parameters	Redox-equilibria as part of GEM	Various, Debye-Hückel, Pitzer, SIT	Advanced, including high temperature applications	Advanced
Reaktoro	GEM[2]	Transport, ODML[4]	Support for various, user extensible	Advanced (non-ideal), user-defined interaction parameters	Redox-equilibria as part of GEM	Various, Debye-Hückel, Pitzer, SIT	Advanced, including high temperature applications	Advanced
PourPy	LMA[1], focus on Pourbaix diagrams	None	Custom, user extensible	No	Redox equilibria with Nernst equation	No	No	No

[1]Law of mass action
[2]Gibbs free energy minimization
[3]Vapor-liquid equilibrium
[4]On-demand machine learning

3 State-of-the-art of thermodynamics for corrosion

In the early days of corrosion science, Marcel Pourbaix was a pioneer in applying thermodynamic principles to understand the electrochemical stability of materials. His work led to the development of the Pourbaix Atlas [99], a collection of potential-pH, or so-called Pourbaix diagrams, illustrating the stability of a total of 43 chemical elements, including their regions of immunity, passivity as well as those areas in which corrosion is favorable. This connection between thermodynamic principles and electrochemical processes was a major departure from the empirical methods commonly used in corrosion science at the time. Perhaps due to their intuitive simplicity, these visual representations have become an indispensable tool to teach thermodynamic concepts in corrosion education and, to some extent, in corrosion engineering.

With regard to the corrosion of steel in concrete, the development of geochemical solvers enables modeling calculations, including the phase assemblage of multi-component systems, significantly more complex than those originally considered. Simultaneously, the underlying thermodynamic data of iron and the list of chemical species that may form has been overhauled significantly throughout the past decades [100-102]. In comparison to those species investigated by Pourbaix [99], recent works, including the extensive compilations of Lemire et al. [100, 101], Brown and Ekberg [103] and other application-specific reviews such as the PSI/Nagra Chemical Thermodynamic Database [104, 105], account for the formation of far more solid iron bearing compounds and aqueous complexes. Some most notable additions of particular relevance to the corrosion of steel in concrete are the formation of:

- soluble iron-chloride ($FeCl^+, FeCl^{2+}, FeCl_3(aq), FeCl_4^-$),
- carbonate ($FeCO_3(aq), Fe(CO_3)_2^{2-}, Fe(CO_3)_3^{3-}$) and
- sulfate ($FeSO_4^+$, $FeSO_4(aq)$, $Fe(SO_4)_2^-$),

complexes, as well as the amorphous, highly soluble corrosion products 2- and 6-line ferrihydrite $\left(2l - Fe(OH)_3(s), 6l - Fe(OH)_3(s)\right)$.

In addition to the overhauled set of chemical species considered, recent thermodynamic compilations are based on a precisely defined reference state and make use of internally consistent auxiliary data [106] for chemical species that are involved in the transformation pathways of iron aquatic systems. Consequentially, assessments of the electrochemical stability of steel in concrete based on the traditional Pourbaix diagram do not capture the influence of various complexating ligands on the solubility of iron in the aqueous phase.

The following sections review the state-of-the-art of thermodynamic modeling techniques, highlighting their added value with respect to the concepts emerging in the early days of the discipline and emphasizing some of the major pitfalls currently preventing their broader adoption for the corrosion of steel in concrete.

3.1 The equilibrium solubility and speciation of iron

As previously highlighted in Section 2, the equilibrium composition predicted by thermodynamic modeling

approaches is inherently dependent on the accuracy and completeness of the underlying thermodynamic database – compounds that are not included cannot be predicted to form. Regarding the phase assemblage of solid iron compounds and the speciation of iron in the aqueous phase, the number of species involved far exceed those commonly used to ascertain whether the corrosion of steel in concrete is thermodynamically feasible.

Depending on the electrolyte composition and pH, the solubility and speciation of iron can be governed by the formation of 15 solid iron oxides, oxide hydroxides and hydroxides[a], as well as over 45 aqueous iron complexes [100, 101, 107, 108]. Their formation is generally controlled by the local degree of supersaturation and pH, the temperature, pressure and the presence of other co-reacting species. Solid iron (hydr)oxide phases are further grouped according to the oxidation state of iron in the octahedral position (Fe^{2+}, Fe^{3+}) and their thermodynamic stability, as indicated by their equilibrium constant of formation $\log_{10}\beta^{\circ}$. Within this thermodynamic stability hierarchy, the formation of the well-ordered compounds goethite ($\alpha - FeOOH(s)$) and hematite ($\alpha - Fe_2O_3(s)$) is favored over the formation of amorphous ferrihydrites [107]. The speciation of iron on the other hand is primarily controlled by the solution pH [109]. In the $Fe(II) - H_2O$ system, iron is present in the form of Fe^{2+} and the Fe(II) hydrolysis products $FeOH^+$, $Fe(OH)_2(aq)$ and $Fe(OH)_3^-$ depending on the pH. In the $Fe(III) - H_2O$ on the other hand, the solubility of iron is determined by Fe^{3+}, the Fe(III) hydrolysis products $FeOH^{2+}$, $Fe(OH)_2^+$, $Fe(OH)_3(aq)$, $Fe(OH)_4^-$ and the polymeric iron species $Fe_2(OH)_2^{4+}$ and $Fe_3(OH)_4^{5+}$. Whilst the ferrous (Fe^{2+}) and the ferric (Fe^{3+}) cation are the most dominant aqueous iron complexes at acidic pH, the solubility of iron is controlled by the formation of $Fe(OH)_3^-$ and $Fe(OH)_4^-$ in alkaline conditions. For a detailed account of the pH-dependent solubility and speciation of the $Fe - H_2O$ system, the reader is referred to Furcas [107]. In addition to these hydrolysis products, both the ferrous and ferric cation can complexate with a broad range of anionic species that are commonly present in the pore solution of hardened concrete. Aqueous Fe(II) and Fe(III) chloride complexes are preferentially stabilized at acidic conditions [100, 101, 109, 110], e.g., such that may be achieved in the absence of a local cathodic reaction in corrosion pits [111, 112]. Their contribution to the solubility of iron at the pH characteristic to the pore solution of concrete is negligible [107, 109].

It has recently been demonstrated that the solubility of Fe(II) is dominated by the formation of aqueous iron carbonate complexes in circumneutral (pH = 9.0) to alkaline (pH = 12.5) conditions. These complexes, including $FeCO_3(aq)$ and $Fe(CO_3)_2^{2-}$, compete with the formation of the hydrolysis products $FeOH^+$ and $Fe(OH)_2(aq)$, accounting for more than 80% of the total dissolved Fe(II) at carbonate concentrations approaching 1×10^{-1} M [107]. Apart from hitherto characterized iron chloride and carbonate complexes, a number of publications further suggest that the solubility of Fe(III) is elevated in the presence of dissolved silicates and carbonates at highly alkaline pH [109, 113, 114]. The presence of Si can further lead to the formation of solid iron silicates, competing with the precipitation of iron (hydr)oxide phases at $T = 50$ °C on the surface of corroding iron and in the aqueous medium in the vicinity of the metal-electrolyte interface [115, 116]. In the light of these competing chemical interactions and their pivotal influence on the dissolution kinetics, the speciation of iron in the aqueous phase and the formation of corrosion products, it is essential to consider their collective influence when evaluating the electrochemical stability of steel in concrete.

One of the key assumptions made to construct the potential- and pH-dependent phase transitions visualized in the classical Pourbaix diagram is that the concentration of iron in the electrolyte is fixed to a constant value, e.g., $[Fe] = 10^{-5}$ M to $[Fe] = 1$ M [99], for all dissolved iron complexes, irrespective of their pH-dependent predominance or oxidation state. Whilst it is indeed thermodynamically possible for some corrosion products to be in equilibrium with such high aqueous iron concentrations, their total solubility is heavily influenced by the pH. In the $Fe(II) - H_2O$ system, the solubility of iron, as controlled by the formation of $Fe(OH)_2(s)$ varies from approx. $[Fe] = 10^{-1}$ M at pH = 7.0 to $[Fe] = 10^{-8}$ M at pH = 11.2 [109]. The total solubility of Fe(III)-complexes on the other hand approaches $[Fe] = 10^{-1}$ M at pH = 2.0 in equilibrium with the amorphous corrosion product 2-line ferrihydrite and can decrease to values as low as $[Fe] = 10^{-12}$ M at pH = 8.0, considering the formation of the crystalline corrosion product goethite [107, 109]. In the light of these ample deviations in the concentration of iron across different oxidation states as well as the aforementioned pH-dependent speciation of Fe(II)- and Fe(III)-complexes, it can be concluded that the general assumption of a constant iron concentration is inadequate.

3.2 The electrochemical stability of iron revised – using modern thermodynamic modeling techniques

Under consideration of the broad range of aqueous and solid iron-bearing species commonly formed in the conditions characteristic to the pore solution of cementitious media, the electrochemical stability of iron can be evaluated using state-of-the-art Gibbs free energy minimization techniques. Figure 2 compares the resultant electrochemical stability regions of various compounds, as computed using the modeling package Reaktoro (Figure 2a) to those obtained from traditional LMA and Nernst Equation calculations [99].

[a] Hereafter collectively referred to as iron (hydr)oxides.

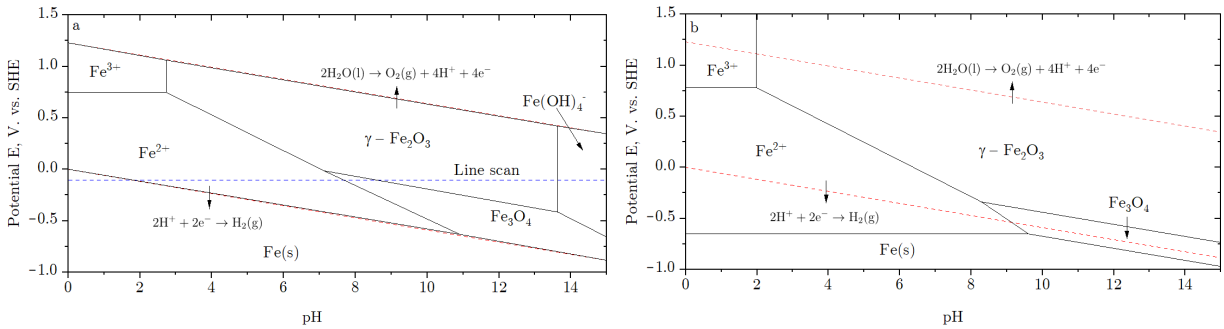

Figure 2. The electrochemical stability of iron-bearing compounds at $T = 298.15$ K as a function of the potential E in V vs. SHE and the pH, as computed using the thermodynamic modeling solver Reaktoro [68] (Figure 2a) and via the software package PourPy [69] (Figure 2b). All simulations assumed a total iron and carbonate content of $[Fe] = 1 \times 10^{-6}$ M and $[C] = 1 \times 10^{-2}$ M, respectively. Modeling calculations were performed, considering the formation of the solid iron compounds $Fe(OH)_2(s)$, $Fe_3O_4(s)$, γ-$Fe_2O_3(s)$ and aqueous complexes Fe^{2+}, $FeOH^+$, $Fe(OH)_2(aq)$, $Fe(OH)_3^-$, Fe^{3+}, $FeOH^{2+}$, $Fe(OH)_2^+$, $Fe(OH)_3(aq)$, $Fe(OH)_4^-$, $Fe_2(OH)_2^{4+}$, $Fe_3(OH)_4^{5+}$, $FeCO_3(aq)$, and $Fe(CO_3)_2^{2-}$, using the thermodynamic data published in Furcas et al. [109] and Furcas et al. [118] .

Simulations were performed on an equally spaced 20×100 potential-pH grid, ranging from pH $= 0$ to 15 and $E = -1.0$ to 1.5 V vs. the standard hydrogen electrode (SHE). The modeling system was adjusted to contain a total elemental concentration of $[Fe] = 1 \times 10^{-6}$ M, $[C] = 1 \times 10^{-2}$ M, i.e. matching the approximate dissolved aqueous carbonate concentration in the pore solution of cementitious systems [117] as well as $[NaCl] = 1 \times 10^{-2}$ M to ensure simulation stability.

It can be recognized that the corrosion regime of iron, i.e. the combined potential-pH space in which aqueous iron species (Fe^{2+}, Fe^{3+}) are predominant, as predicted by Gibbs free energy minimization approaches (Figure 2a), stretches to far higher pH values than the stability regime bound by traditional law of mass action and Nernst equation-type lines (Figure 2b). In addition, it is found that the Fe(III) hydrolysis product $Fe(OH)_4^-$ exhibits significant electrochemical stability, rivalling the formation of all solid iron oxides considered at pH > 13.6. The obtained differences in the size of the passivity regime can be traced back directly to the calculation methodology and underlying model assumptions of both approaches. Whilst the electrochemical stability diagram constructed using rigid thermodynamic modelling techniques (Figure 2a) accounts for the pH-dependent solubility of iron-bearing compounds, the classical Pourbaix diagram (Figure 2b) assumes a constant, pH-independent concentration of iron in the electrolyte. The classical Pourbaix diagram is hence unable to capture the ample reduction in the total concentration of iron in solution towards circumneutral pH. This crucial simplification provides a prospective explanation as to why the onset of steel passivity at potentials characteristic to aerated concrete [119], estimated using classical Pourbaix diagram [99], does not align with field observations. In addition to the pH-dependent formation of solid iron-bearing phases, the assumption of a constant aqueous iron concentration bears the risk of misestimating other competing reactive transport processes, including the kinetics of the anodic dissolution of iron or its subsequent uptake by cementitious phases. As both of the latter depend on the local concentration of the divalent and trivalent Fe cation, it can be concluded that Gibbs free energy minimization techniques are far more adept at capturing the complex chemical interactions relevant for corrosion and corrosion-related damage in reinforced concrete structures.

The power of state-of-the-art thermodynamic modeling techniques, as well as their advantages over Nernst equation-based approaches, is further demonstrated by the breadth of information they can provide. Whilst the classical Pourbaix diagram visualizes the potential-pH stability regime of only those species that are thermodynamically predominant, Gibbs free energy minimization approaches provide detailed insights into the potential- and pH-dependent concentrations of all species considered. Figure 3 illustrates the molar fractions of various predominant compounds (Figure 3a) an aqueous iron-bearing complexes (Figure 3b), computed across a parametrized line scan from pH 0 to 15, at a constant potential of $E = -0.1$ V vs. SHE (compare Figure 2a, blue, dashed line). It can be recognized that the transition between the corrosion and passivation regime, as visualized by a sharp border in classical Pourbaix diagrams, entails an entire set of aqueous iron complexes that are otherwise hidden within the stability domain of Fe^{2+} and $Fe_3O_4(s)$ (Figure 3a). Though not thermodynamically predominant, some of these complexes, including $Fe(OH)_2^+$, $Fe(OH)_3(aq)$ and $Fe(OH)_4^-$, contribute significantly to the pH-dependent equilibrium composition of iron in the $Fe - H_2O$ system (Figure 3b). It is further evident that the transition of one iron-bearing compound to another, e.g., from of Fe^{2+} to $Fe_3O_4(s)$, proceeds significantly smoother than visually conveyed in the thermodynamic predominance diagrams displayed in Figure 2. Approaching their transition point at pH 7.5, the total molar fraction of $Fe_3O_4(s)$ gradually increases (Figure 3a, red line) at the expense of the amount of soluble Fe^{2+} (Figure 3a, black line). Whilst the ferric cation ceases to be thermodynamically predominant at pH > 7.5, it remains stable within the predominance region of $Fe_3O_4(s)$ up to pH 9.0. Likewise, as the total solubility of Fe increases towards highly alkaline conditions [109], the total molar fraction of the Fe(III) hydrolysis product $Fe(OH)_4^-$ gradually increases (Figure 3a, grey line), whilst the relative contribution of the corrosion product γ-$Fe_2O_3(s)$ experiences a smooth decrease (Figure 3a, blue line).

The additional consideration of dissolved carbonates in quantities characteristic to cementitious media further exemplifies the power of modern thermodynamic modeling techniques to simulate compositional changes due to environmental variations. It is demonstrated that the solubility of iron is influenced by the formation of $FeCO_3(aq)$ and $Fe(CO_3)_2^{2-}$ (Figure 3b, red and blue lines). Despite their significant contributions to the aqueous molar fraction of iron, neither of the Fe(II) carbonate complexes is thermodynamically predominant in comparison to Fe^{2+}, $Fe(OH)_4^-$ or any of the solid iron-bearing phases considered (Figure 3a). Consequently, both $FeCO_3(aq)$ and $Fe(CO_3)_2^{2-}$ do not appear on the classical Pourbaix diagram of iron. Nevertheless, under the continual carbonation of hardened concrete, it is anticipated that these complexes stabilize in the chemical near-field of the steel concrete interface. Consequentially, their formation could impact both the dissolution of steel in carbonated concrete [107] as well as subsequent reaction pathways that lead to the precipitation of corrosion products and the uptake of iron into cementitious phases [14].

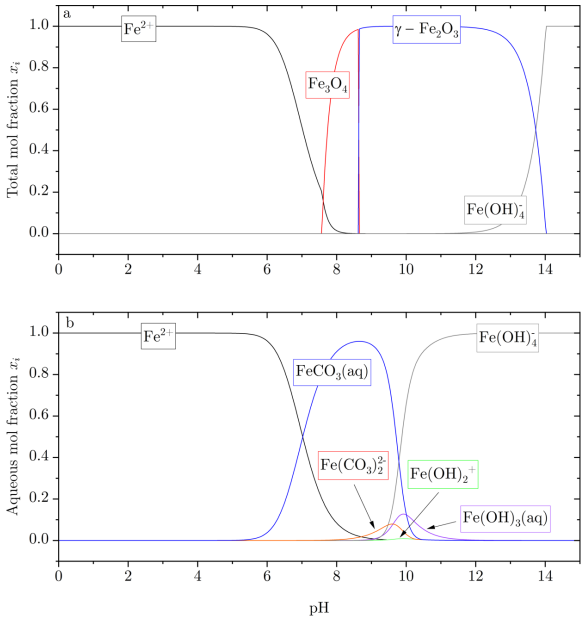

Figure 3. The mol fraction of all thermodynamically predominant species across a line scan performed over the entire pH space at $E = -0.1$ V vs. SHE (compare Figure 2), w.r.t the total iron concentration. Figure 3a displays the mol fraction of all predominant compounds whilst Figure 3b shows all thermodynamically stable aqueous species across the same potential and pH space.

3.3 Thermodynamics and kinetics – opposing approaches?

While thermodynamic models can determine whether corrosion is *possible*, they also operate under the assumption that the system will eventually reach equilibrium. Consequentially, they do not provide any information on the time-dependent availability of reactants at the metal-electrolyte interface or the rate at which equilibrium is approached.

Kinetic modeling approaches on the other hand ascertain the rate at which the electrochemical degradation occurs. These models incorporate reaction kinetics, transport phenomena, i.e. the diffusion or migration of reactants and products, and other surface phenomena including the adsorption and desorption of species onto the electrode surface. Accounting for the time-dependent availability of chemical species, kinetic models are crucial for understanding how quickly corrosion progresses in real-world conditions where a system is often far from equilibrium.

Although both techniques are widely recognized as crucial components of the modeling toolbox used to investigate corrosion of metals, they are regarded as distinct. Their apparent opposition arises from the fact that a material may be thermodynamically prone to corrosion, but kinetic barriers, e.g., diffusion limitations or the formation of a passive film, may attenuate the rate of material degradation within a relevant operational timeframe. Despite this perceived contradiction, it is important to clarify that these techniques are not opposing, but rather complementary. Thermodynamics determines whether a reaction can happen at all or not, while kinetic determines the speed at which possible reactions can happen. Consider the Arrhenius-type relationship between the current density i and the electrode overpotential η, as described by the Butler-Volmer Equation

$$i = i_0 \left[\exp\left(\frac{\alpha_a n F \eta}{RT}\right) - \exp\left(\frac{-\alpha_c n F \eta}{RT}\right)\right], \quad (1)$$

where i_o is the exchange current density, α_a and α_c are the anodic and cathodic charge transfer coefficients, n is the number of electrons exchanged, T represents the temperature in degree Kelvin and R and F are the ideal gas and Faraday constant. The overpotential

$$\eta = E - E_0 \quad (2)$$

is a measure of the deviation from the thermodynamically defined equilibrium potential E_0, driving the electrochemical reaction forward, towards the oxidation of the metal ($\eta > 0$), or favouring the reduction of metal cations in the immediate vicinity of the electrode ($\eta < 0$). In either scenario, the Gibbs free energy change of the reaction ΔG_r, the cell potential $E = \frac{-\Delta G_r}{nF}$, and consequentially the current density i depend on the activity of all chemical species taking part in the reaction. The thermodynamic principles defining the driving force for corrosion to occur are thus hard coded into the mathematical description of electrochemical kinetics.

4 Opportunities and research perspectives

In the light of the most recent analytical and computational advancements, several challenges remain to be addressed to fully harness the potential of thermodynamic modeling techniques for the corrosion of steel in concrete, many of which originate from the competition between thermodynamically and kinetically controlled processes occurring at the steel-concrete interface. The steel-concrete interface is a complex domain with interacting microscopic features (e.g., pores, mill scale, pre-existing rust layers, cracks, crevices) and chemical states (e.g., varying degrees of saturation, phases and microstructure different from bulk

concrete, varying ionic compositions) [120]. One of the key challenges involved is the accurate modeling of various thermodynamic and kinetic factors affecting the distribution of Fe(II) and Fe(III), both in the aqueous and solid phase. Corrosion of steel in concrete proceeds via the anodic dissolution of Fe and the simultaneous cathodic reaction, often involving the generation of OH^-. Depending on the pH and the activity of anions in the pore solution, the released Fe^{2+} may form complexes, oxidize to Fe(III) over time, diffuse away from the steel interface or precipitate as Fe(II) solids [121]. The Fe(III) species formed may also form complexes with anions in the pore solution [109], diffuse away from the steel interface, and precipitate as solid Fe(III) (hydr)oxides, which can further transform into thermodynamically more stable phases [122]. Despite the importance of these kinetic phenomena, experimental investigation of processes near the steel-concrete interface is rather challenging and requires innovative approaches and computational techniques.

Reactive-transport modeling of the steel-concrete interface provides such an opportunity to overcome experimental limitations. Reactive transport models, though few, studying the evolution of corrosion in cementitious materials do exist in the literature. Some of these models also couple thermodynamic modeling algorithms (e.g., Gibbs free energy minimization or LMA) with numerical solution algorithms for solving the governing equations for transport [30, 31]. However, most of these models do not currently consider all the relevant thermodynamic data for aqueous and solid Fe phases. Considering the importance of accurate and internally consistent thermodynamic data as outlined in Section 2, it is crucial to complete the existing data set of iron by adding and characterizing various ferrous and ferric carbonate and silicon complexes that are hypothesized to stabilize at alkaline pH [109, 113]. When combined with recent efforts in characterizing the microstructural domains near the steel-interface [123] to create representative domains for reactive-transport simulations, the foundations for the next generation of service life prediction tools for reinforced concrete structures can be established. Figure 4 illustrates the set of key milestones towards the development of these next-generation prediction tools.

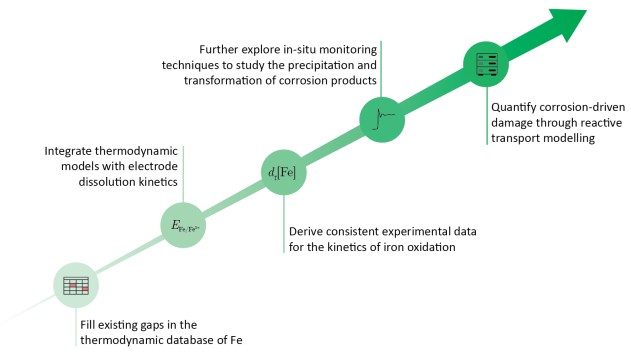

Figure 4. The set of key milestones required for the development of next-generation service-life prediction tools, leveraging the full potential of kinetic, thermodynamic and coupled reactive transport modeling techniques, ultimately contributing to more reliable assessment of the corrosion state of steel in reinforced concrete structures.

In addition to the microstructure, it has been shown that the fate of Fe in corroding steel-reinforced concrete is strongly influenced by the oxidation rate of Fe(II) to Fe(III). The oxidation of Fe(II) to Fe(III) entails multiple concurrent oxidation reactions involving different Fe(II) and Fe(III) species, each with a different kinetic rate constant [124, 125]. The rate of each oxidation reaction is influenced by variables such as pH, dissolved oxygen concentration, and pore solution composition [126-128]. Thermodynamic modeling can help in deciphering the speciation of aqueous Fe(II) and Fe(III) and allow us to numerically estimate the effective rate of each of the underlying oxidation reactions. However, these estimates often vary by a few orders of magnitude due to lack of consistent experimentally derived kinetic rate constants. In the absence of an internally consistent description of the concurrent oxidation reactions, model predictions could lead to significant discrepancies in the concentration of dissolved Fe(II) and Fe(III) complexes either overpredicting the amount of ferrous species formed and underestimating the Fe(III) activity, or the other way round. This misrepresentation of the prevailing chemical environment would in turn affect the kinetics of Fe^{2+} dissolution at the SCI (compare Section 3.3.) as well as the rate of corrosion product formation under partial equilibrium [122, 129].

Another factor that influences the rate of $Fe^{(0)}$ dissolution is the degree of pore water saturation in the vicinity of the SCI. Moisture plays a critical role in the degradation of steel reinforcement, acting both as a medium for the flow of current between anode and cathode as well as the transport of corrosive species to the dissolution site. It is well known that the corrosion rates of steel in a broad range of cementitious binders exposed to high relative humidity (90 to 100% RH) or immersed in water can surge by 1 to 2 orders of magnitude compared to systems in moderately dry environments (30 to 50 % RH) [130-134]. Apart from the thermodynamic and kinetic considerations related to (electro)chemical reactions, next generation service life prediction tools are required account for the dynamic influence of the prevailing degree of pore saturation on the rate of steel dissolution, thereby affecting other competing reactive transport phenomena discussed in this section.

There is also a need for new ways of studying the kinetic processes near the steel-electrolyte interface. Traditional in-situ electrochemical techniques [135] do not allow to study the location of formation and type of solid reaction products in the electrolyte. Ex-situ surface characterization techniques of corrosion products (e.g., Raman spectroscopy or X-ray photoelectron spectroscopy) focus on the changes on the metal surface, but do not work well to study precipitates and their undisturbed transformations over time in the region near the metal-electrolyte interface. Therefore, there is a dire need for new techniques that can provide in-situ kinetic information on the long-term processes near the steel-electrolyte interface. A recent study by Albert et al. [136] presented such a new experimental approach which is based on a glass capillary, in which precipitation of corrosion products in the aqueous phase adjacent to the steel surface can be monitored over time with optical microscopy and

chemically and microscopic synchrotron-based techniques. Moreover, quantification of precipitates through X-ray transmission measurements provides in-situ corrosion rates. Another opportunity to develop fundamental understanding on kinetic processes is provided by the recent advances in utilizing atomistic modeling techniques. For instance, reactive-force field molecular dynamics and density functional theory have been shown to be highly beneficial in developing fundamental understanding of corrosion processes near metal-electrolyte interface to fundamentally explain concepts such as passivation, chloride-induced breakdown of passive films, speciation of iron in electrolytes, and the role of ionic state on reaction kinetics [25, 26, 137].

Applying thermodynamic modeling principles to develop fundamental understanding for corrosion of steel reinforcement in concrete has practical importance, as demonstrated by Küter [138]. By accounting for the formation of soluble complexes, e.g., those that play a role in the propagation of chloride-induced corrosion [138, 139], the devised approach aims to thermodynamically describe the diverse corrosion states of steel in concrete. Küter [138] showed that it is possible to assess available countermeasures to mitigate reinforcement corrosion, and further, to develop theoretical concepts for new effective and cost-efficient countermeasures for both new and existing structures. Examples of how thermodynamic principles could be used to mitigate reinforcement corrosion include tailored surface modification of the steel reinforcement and development of new concepts for sacrificial anodes to be used in cathodic protection systems.

In conclusion, thermodynamic modeling is expected to play a significant role in the low-carbon vision of the concrete industry which promotes the use of low-clinker binders with high limestone replacement, extensive use of traditional and alternative supplementary cementitious materials (SMS), and non-clinker based alternative cements or alkali activated binders. These low-clinker systems have significant implications on steel corrosion in concrete. First, these systems typically have a low pH buffer capacity due to reduced or eliminated $Ca(OH)_2$ in the cementitious matrix. Second, cementitious reactions or externally-induced chemical reactions (e.g., carbonation) in these systems can result in pore solution chemistries that can destabilize passivity of steel and increase corrosion rates. Third, the ability of these mixtures to bind aggressive species such as chlorides could be considerably different from the conventional concrete. Finally, physical binding of anions and cations from the pore solution by the hardened cementitious phases (e.g., C-S-H, C-A-S-H, etc.) of these low-clinker mixtures could lead to unexpected outcomes with respect to key aspects of pore solution composition related to reinforcement corrosion such as pH, Cl^-/OH^- ratio, alkali content, and electrical resistivity. Fortunately, thermodynamic modeling provides an unmatched opportunity to address these uncertainties as it provides a generic framework for quantifying solid and aqueous phases, indifferent to the type of cementitious materials used.

Acknowledgments

This work is supported by the Swiss National Science Foundation project no. 10000099: PRINCE.

Authorship statement (CRediT)

Fabio Enrico Furcas: Conceptualization, Methodology, Software, Validation, Formal analysis, Investigation, Data curation, Writing – Original Draft, Visualization. **Barbara Lothenbach:** Conceptualization, Methodology, Validation, Formal analysis, Investigation, Data curation, Writing – Review & Editing, Funding acquisition, Supervision. **Shishir Mundra:** Conceptualization, Methodology, Validation, Formal analysis, Investigation, Data curation, Writing – Review & Editing, Supervision. **O. Burkan Isgor:** Conceptualization, Methodology, Validation, Formal analysis, Investigation, Data curation, Writing – Review & Editing, Supervision. **Mette R. Geiker:** Conceptualization, Methodology, Validation, Formal analysis, Investigation, Data curation, Writing – Review & Editing. **Ueli M. Angst:** Conceptualization, Methodology, Validation, Formal analysis, Investigation, Data curation, Writing – Review & Editing, Funding acquisition, Supervision.

References

[1] Béton, F.I.d., Model code for service life design. fib bulletin. 2006, Lausanne: Fédération Internationale du Béton.

[2] Angst, U.M., O.B. Isgor, C.M. Hansson, A. Sagüés, and M.R. Geiker, Beyond the chloride threshold concept for predicting corrosion of steel in concrete. Applied Physics Reviews, 2022. 9(1). https://doi.org/10.1063/5.0076320

[3] Melchers, R.E. and C.Q. Li, Phenomenological modeling of reinforcement corrosion in marine environments. ACI Materials Journal, 2006. 103(1): p. 25. https://doi.org/10.14359/15124

[4] Yilmaz, D. and U. Angst, Korrosionsbedingte Kosten an Ingenieurbauwerken im Schweizer Straßennetz. Beton- und Stahlbetonbau, 2020. 115(6): p. 448-458. https://doi.org/10.1002/best.202000004

[5] Koch, G., Cost of corrosion, in Trends in oil and gas corrosion research and technologies. 2017, Woodhead Publishing. p. 3-30. https://doi.org/10.1016/B978-0-08-101105-8.00001-2

[6] Habert, G., S.A. Miller, V.M. John, J.L. Provis, A. Favier, A. Horvath, and K.L. Scrivener, Environmental impacts and decarbonization strategies in the cement and concrete industries. Nature Reviews Earth & Environment, 2020. 1(11): p. 559-573. https://doi.org/10.1038/s43017-020-0093-3

[7] Scrivener, K.L., V.M. John, and E.M. Gartner, Eco-efficient cements: Potential economically viable solutions for a low-CO2 cement-based materials industry. Cement and Concrete Research, 2018. 114: p. 2-26. https://doi.org/10.1016/j.cemconres.2018.03.015

[8] Favier, A., C. De Wolf, K. Scrivener, and G. Habert, A sustainable future for the European Cement and Concrete Industry: Technology assessment for full decarbonisation of the industry by 2050. 2018, ETH Zurich.

[9] Cembureau, Cementing the European Green Deal. 2020, The European Cement Association Brussels, Belgium.

[10] Cement, G., GCCA Climate Ambition Statement-Towards Carbon Neutral Concrete. Global Cement and Concrete Association, 2020.

[11] Flatt, R.J. and T. Wangler, On sustainability and digital fabrication with concrete. Cement and Concrete Research, 2022. 158: p. 106837. https://doi.org/10.1016/j.cemconres.2022.106837

[12] Wangler, T., E. Lloret, L. Reiter, N. Hack, F. Gramazio, M. Kohler, M. Bernhard, B. Dillenburger, J. Buchli, and N. Roussel, Digital concrete: opportunities and challenges. Rilem technical letters, 2017. 1(1): p. 67-75. https://doi.org/10.21809/rilemtechlett.2016.16

[13] Gartner, E. and T. Sui, Alternative cement clinkers. Cement and Concrete Research, 2018. 114: p. 27-39. https://doi.org/10.1016/j.cemconres.2017.02.002

[14] Angst, U.M., Steel corrosion in concrete-Achilles' heel for sustainable concrete? Cement and Concrete Research, 2023. 172: p. 107239. https://doi.org/10.1016/j.cemconres.2023.107239

[15] Otieno, M.B., H.D. Beushausen, and M.G. Alexander, Modelling corrosion propagation in reinforced concrete structures-A critical review. Cement and Concrete Composites, 2011. 33(2): p. 240-245. https://doi.org/10.1016/j.cemconcomp.2010.11.002

[16] Jamali, A., U. Angst, B. Adey, and B. Elsener, Modeling of corrosion-induced concrete cover cracking: A critical analysis. Construction and Building Materials, 2013. 42: p. 225-237. https://doi.org/10.1016/j.conbuildmat.2013.01.019

[17] Isgor, O.B. and W.J. Weiss, A nearly self-sufficient framework for modelling reactive-transport processes in concrete. Materials and Structures, 2019. 52(1): p. 1-17. https://doi.org/10.1617/s11527-018-1305-x

[18] Rossi, E., S. Governo, M. Shakoorioskooie, Q. Zhan, S. Mundra, D. Mannes, A. Kaestner, and U. Angst, X-ray computed tomography to observe the presence of water in macropores of cementitious materials. RILEM Technical Letters, 2023. 8: p. 165-175. https://doi.org/10.21809/rilemtechlett.2023.190

[19] Albert, C.C., S. Mundra, D. Ferreira Sanchez, F.E. Furcas, A.D. Rajyaguru, O.B. Isgor, D. Grolimund, and U.M. Angst, Microscale chemical imaging to characterize and quantify corrosion processes at the metal-electrolyte interface. npj Materials Degradation, 2024. 8(1): p. 116. https://doi.org/10.1038/s41529-024-00534-x

[20] Mundra, S., E. Rossi, L. Malenica, M. Pundir, and U.M. Angst, Precipitation of corrosion products in macroscopic voids at the steel-concrete interface--observations, mechanisms and research needs. arXiv preprint arXiv:2408.05028, 2024. https://doi.org/10.1617/s11527-025-02614-z

[21] Ghods, P., O. Isgor, G. Carpenter, J. Li, G. McRae, and G. Gu, Nano-scale study of passive films and chloride-induced depassivation of carbon steel rebar in simulated concrete pore solutions using FIB/TEM. Cement and Concrete Research, 2013. 47: p. 55-68. https://doi.org/10.1016/j.cemconres.2013.01.009

[22] Gunay, H.B., P. Ghods, O.B. Isgor, G.J.C. Carpenter, and X.H. Wu, Characterization of atomic structure of oxide films on carbon steel in simulated concrete pore solutions using EELS. Applied Surface Science, 2013. 274: p. 195-202. https://doi.org/10.1016/j.apsusc.2013.03.014

[23] Ghods, P., O. Isgor, J. Brown, F. Bensebaa, and D. Kingston, XPS depth profiling study on the passive oxide film of carbon steel in saturated calcium hydroxide solution and the effect of chloride on the film properties. Applied Surface Science, 2011. 257(10): p. 4669-4677. https://doi.org/10.1016/j.apsusc.2010.12.120

[24] Ghods, P., O.B. Isgor, F. Bensebaa, and D. Kingston, Angle-resolved XPS study of carbon steel passivity and chloride-induced depassivation in simulated concrete pore solution. Corrosion Science, 2012. 58: p. 159-167. https://doi.org/10.1016/j.corsci.2012.01.019

[25] DorMohammadi, H., Q. Pang, P. Murkute, L. Árnadóttir, and O.B. Isgor, Investigation of chloride-induced depassivation of iron in alkaline media by reactive force field molecular dynamics. npj Materials Degradation, 2019. 3(1): p. 1-11. https://doi.org/10.1038/s41529-019-0081-6

[26] DorMohammadi, H., Q. Pang, L. Árnadóttir, and O.B. Isgor, Atomistic simulation of initial stages of iron corrosion in pure water using reactive molecular dynamics. Computational Materials Science, 2018. 145: p. 126-133. https://doi.org/10.1016/j.commatsci.2017.12.044

[27] Pundir, M., D.S. Kammer, and U. Angst, An FFT-based framework for predicting corrosion-driven damage in fractal porous media. Journal of the Mechanics and Physics of Solids, 2023. 179: p. 105388. https://doi.org/10.1016/j.jmps.2023.105388

[28] Lothenbach, B., D. Damidot, T. Matschei, and J. Marchand, Thermodynamic modelling: state of knowledge and challenges. Advances in Cement Research, 2010. 22(4): p. 211-223. https://doi.org/10.1680/adcr.2010.22.4.211

[29] Damidot, D., B. Lothenbach, D. Herfort, and F. Glasser, Thermodynamics and cement science. Cement and Concrete Research, 2011. 41(7): p. 679-695. https://doi.org/10.1016/j.cemconres.2011.03.018

[30] Azad, V.J., C. Li, C. Verba, J.H. Ideker, and O.B. Isgor, A COMSOL-GEMS interface for modeling coupled reactive-transport geochemical processes. Computers & Geosciences, 2016. 92: p. 79-89. https://doi.org/10.1016/j.cageo.2016.04.002

[31] Isgor, O.B. and W.J. Weiss, A nearly self-sufficient framework for modelling reactive-transport processes in concrete. Materials and Structures, 2019. 52(1). https://doi.org/10.1617/s11527-018-1305-x

[32] Lothenbach, B. and F. Winnefeld, Thermodynamic modelling of the hydration of Portland cement. Cement and Concrete Research, 2006. 36(2): p. 209-226. https://doi.org/10.1016/j.cemconres.2005.03.001

[33] Winnefeld, F. and B. Lothenbach, Hydration of calcium sulfoaluminate cements-Experimental findings and thermodynamic modelling. Cement and Concrete Research, 2010. 40(8): p. 1239-1247. https://doi.org/10.1016/j.cemconres.2009.08.014

[34] De Weerdt, K., M.B. Haha, G. Le Saout, and B. Lothenbach, Hydration mechanisms of ternary Portland cements containing limestone powder and fly ash. Cement and Concrete Research, 2011. 41(3): p. 279-291. https://doi.org/10.1016/j.cemconres.2010.11.014

[35] Lothenbach, B., G. Le Saout, E. Gallucci, and K. Scrivener, Influence of limestone on the hydration of Portland cements. Cement and Concrete Research, 2008. 38(6): p. 848-860. https://doi.org/10.1016/j.cemconres.2008.01.002

[36] Lothenbach, B., T. Matschei, G. Möschner, and F.P. Glasser, Thermodynamic modelling of the effect of temperature on the hydration and porosity of Portland cement. Cement and Concrete Research, 2008. 38(1): p. 1-18. https://doi.org/10.1016/j.cemconres.2007.08.017

[37] Haha, M.B., G. Le Saout, F. Winnefeld, and B. Lothenbach, Influence of activator type on hydration kinetics, hydrate assemblage and microstructural development of alkali activated blast-furnace slags. Cement and Concrete Research, 2011. 41(3): p. 301-310. https://doi.org/10.1016/j.cemconres.2010.11.016

[38] Bharadwaj, K., W.J. Weiss, and O.B. Isgor, Towards performance-based specifications for fly ash and natural pozzolans-Insights from a Monte-Carlo based thermodynamic modeling framework. Cement and Concrete Research, 2023. 172. https://doi.org/10.1016/j.cemconres.2023.107230

[39] Mcalexander, M., K. Bharadwaj, W.J. Weiss, and O.B. Isgor, Waterglass-based clinker-free cementitious systems. Construction and Building Materials, 2024. 417. https://doi.org/10.1016/j.conbuildmat.2024.135317

[40] Bharadwaj, K., O.B. Isgor, and W.J. Weiss, Optimizing the Carbon Footprint of Performance-Engineered Concrete Mixtures. Transportation Research Record, 2024. 2678(10): p. 1422-1440. https://doi.org/10.1177/03611981241236792

[41] Angst, U.M., Challenges and opportunities in corrosion of steel in concrete. Materials and Structures, 2018. 51(1): p. 1-20. https://doi.org/10.1617/s11527-017-1131-6

[42] Lothenbach, B., D. Kulik, T. Matschei, M. Balonis, L.G. Baquerizo, B.Z. Dilnesa, G.D. Miron, and D. Myers, Cemdata18: A chemical thermodynamic database for hydrated Portland cements and alkali-activated materials. Cement and Concrete Research, 2019. 115: p. 472-506. https://doi.org/10.1016/j.cemconres.2018.04.018

[43] Loser, R., B. Lothenbach, A. Leemann, and M. Tuchschmid, Chloride resistance of concrete and its binding capacity - comparison between experimental results and thermodynamic modeling. Cement and Concrete Composites, 2010. 32(1): p. 34-42. https://doi.org/10.1016/j.cemconcomp.2009.08.001

[44] De Weerdt, K., E. Bernard, W. Kunther, M.T. Pedersen, and B. Lothenbach, Phase changes in cementitious materials exposed to saline solutions. Cement and Concrete Research, 2023. 165: p. 107071. https://doi.org/10.1016/j.cemconres.2022.107071

[45] Babushkin, V.I., O.P. Matveev, and O.P. Mčedlov-Petrosjan, Thermodinamika Silikatov. 1965, Moskau: Strojisdat.

[46] Nikushchenko, V.M., V.S. Khotimchenko, P.F. Rumyantsev, and A.I. Kalinin, Determination of the standard free energies of formation of calcium hydroxyaluminates. Cement and Concrete Research, 1973. 3: p. 625-632. https://doi.org/10.1016/0008-8846(73)90099-9

[47] Barret, P., D. Bertrandie, and D. Beau, Calcium hydrocarboaluminate, carbonate, alumina gel and hydrated aluminates solubility diagram calculated in equilibrium with CO2g and with Na+aq ions. Cement and Concrete Research, 1983. 13: p. 789-800. https://doi.org/10.1016/0008-8846(83)90080-7

[48] Reardon, E.J., An ion interaction model for the determination of chemical equilibria in cement/water systems. Cement and Concrete Research, 1990. 20: p. 175-192. https://doi.org/10.1016/0008-8846(90)90070-E

[49] Neall, F.B., Modelling of the near-field chemistry of the SMA repository at the Wellenberg Site. 1994, PSI: Villigen, Switzerland. p. 45.

[50] Damidot, D., S. Stronach, A. Kindness, M. Atkins, and F.P. Glasser, Thermodynamic investigation of the CaO-Al2O3-CaCO3-H2O closed system at 25° C and the influence of Na2O. Cement and Concrete Research, 1994. 24(3): p. 563-572. https://doi.org/10.1016/0008-8846(94)90145-7

[51] Bourbon, X., Chemical conceptual model for cement based materials ~ mineral phases and thermodynamic data. 2003, ANDRA Technical Report C.NT.ASCM.03.026.A.

[52] Reardon, E.J., Problems and approaches to the prediction of the chemical composition in cement/water systems. Waste Management, 1992. 12: p. 221-239. https://doi.org/10.1016/0956-053X(92)90050-S

[53] Bennett, D.G., D. Read, M. Atkins, and F.P. Glasser, A thermodynamic model for blended cements. II: Cement hydrate phases; thermodynamic values and modelling studies. Journal of Nuclear Materials, 1992. 190: p. 315-325. https://doi.org/10.1016/0022-3115(92)90096-4

[54] Matschei, T., B. Lothenbach, and F.P. Glasser, Thermodynamic properties of Portland cement hydrates in the system CaO-Al2O3-SiO2-CaSO4-CaCO3-H2O. Cement and Concrete Research, 2007. 37(10): p. 1379-1410. https://doi.org/10.1016/j.cemconres.2007.06.002

[55] Möschner, G., B. Lothenbach, J. Rose, A. Ulrich, R. Figi, and R. Kretschmar, Solubility of Fe-ettringite (Ca6[Fe(OH)6]2(SO4)3.26H2O). Geochimica et Cosmochimica Acta, 2008. 72(1): p. 1-18. https://doi.org/10.1016/j.gca.2007.09.035

[56] Möschner, G., B. Lothenbach, A. Ulrich, R. Figi, and R. Kretschmar, Solid solution between Al-ettringite and Fe-ettringite (Ca6[Al1-xFex(OH)6]2(SO4)3.26H2O). Cement and Concrete Research, 2009. 39: p. 482-489. https://doi.org/10.1016/j.cemconres.2009.03.001

[57] Schmidt, T., B. Lothenbach, M. Romer, K.L. Scrivener, D. Rentsch, and R. Figi, A thermodynamic and experimental study of the conditions of thaumasite formation. Cement and Concrete Research, 2008. 38(3): p. 337-349. https://doi.org/10.1016/j.cemconres.2007.11.003

[58] Blanc, P., X. Bourbon, A. Lassin, and E. Gaucher, Chemical model for cement-based materials: Temperature dependence of thermodynamic functions for nanocrystalline and crystalline C-S-H phases. Cement and Concrete Research, 2010. 40(6): p. 851-866. https://doi.org/10.1016/j.cemconres.2009.12.004

[59] Blanc, P., X. Bourbon, A. Lassin, and E. Gaucher, Chemical model for cement-based materials: Thermodynamic data assessment for phases other than CSH. Cement and Concrete Research, 2010. 40(9): p. 1360-1374. https://doi.org/10.1016/j.cemconres.2010.04.003

[60] Yan, Y., B. Ma, G.D. Miron, D.A. Kulik, K. Scrivener, and B. Lothenbach, Al uptake in calcium silicate hydrate and the effect of alkali hydroxide. Cement and Concrete Research, 2022. 162: p. 106957. https://doi.org/10.1016/j.cemconres.2022.106957

[61] Lothenbach, B., D. Jansen, Y. Yan, and J. Schreiner, Solubility and characterization of synthesized 11 Å Al-tobermorite. Cement and Concrete Research, 2022. 159: p. 106871. https://doi.org/10.1016/j.cemconres.2022.106871

[62] Lothenbach, B., B. Xu, and F. Winnefeld, Thermodynamic data for magnesium (potassium) phosphates. Applied Geochemistry, 2019. 111: p. 104450. https://doi.org/10.1016/j.apgeochem.2019.104450

[63] Bernard, E., J. Zucha, B. Lothenbach, and U. Mäder, Stability of hydrotalcite (Mg-Al double layer hydroxide) in presence of different anions. Cement and Concrete Research, 2022. 152: p. 106674. https://doi.org/10.1016/j.cemconres.2021.106674

[64] Hirsch, T. and B. Lothenbach, Phase stabilities and thermodynamic properties of crystalline phases in CaO-SiO2-H2O above 100 °C. Cement and Concrete Research, 2024. 177: p. 107412. https://doi.org/10.1016/j.cemconres.2023.107412

[65] Parkhurst, D.L., U.S. Geological Survey Water-Resources Investigations Report. 1995. p. 143.

[66] Kulik, D., T. Wagner, S. Dmytrieva, G. Kosakowski, F. Hingerl, K. Chudnenko, and U. Berner, GEM-Selektor geochemical modeling package: revised algorithm and GEMS3K numerical kernel for coupled simulation codes. Computational Geosciences, 2013. 17(1): p. 1-24. https://doi.org/10.1007/s10596-012-9310-6

[67] Wagner, T., D.A. Kulik, F.F. Hingerl, and S.V. Dmytrieva, GEM-Selektor geochemical modeling package: TSolMod library and data interface for multicomponent phase models. Canadian Mineralogist, 2012. 50: p. 1173-1195. https://doi.org/10.3749/canmin.50.5.1173

[68] Leal, A.M.M. Reaktoro: An open-source unified framework for modeling chemically reactive systems. 2015; Available from: https://reaktoro.org

[69] Korber, A., F.E. Furcas, M. Pundir, D.S. Kammer, and U. Angst, PourPy-A python package to generate potential-pH diagrams. The Journal of Open Source Software, 2024. 9(97): p. 6536. https://doi.org/10.21105/joss.06536

[70] Damidot, D., B. Lothenbach, D. Herfort, and F.P. Glasser, Thermodynamics and cement science. Cement and Concrete Research, 2011. 41(7): p. 679-695. https://doi.org/10.1016/j.cemconres.2011.03.018

[71] Lothenbach, B., Thermodynamic equilibrium calculations in cementitious systems. Materials and Structures, 2010. 43: p. 1413-1433. https://doi.org/10.1617/s11527-010-9592-x

[72] Kulik, D.A., F. Winnefeld, A. Kulik, G.D. Miron, and B. Lothenbach, CemGEMS - an easy-to-use web application for thermodynamic modelling of cementitious materials. RILEM Technical Letters, 2021. 6(0): p. 36-52. https://doi.org/10.21809/rilemtechlett.2021.140

[73] Chen, Y., L.M. de Lima, Z. Li, B. Ma, B. Lothenbach, S. Yin, Q. Yu, and G. Ye, Synthesis, solubility and thermodynamic properties of N-A-S-H gels with various target Si/Al ratios. Cement and Concrete Research, 2024. 180: p. 107484. https://doi.org/10.1016/j.cemconres.2024.107484

[74] Chen, Y., B. Ma, J. Chen, Z. Li, X. Liang, L.M. de Lima, C. Liu, S. Yin, Q. Yu, B. Lothenbach, and G. Ye, Thermodynamic modeling of alkali-activated fly ash paste. Cement and Concrete Research, 2024. 186. https://doi.org/10.1016/j.cemconres.2024.107699

[75] German, A., F. Winnefeld, P. Lura, D. Rentsch, and B. Lothenbach, Hydrous carbonate-containing brucite (HCB) in MgO/hydromagnesite blends. Cement and Concrete Research, 2023. 173: p. 107304. https://doi.org/10.1016/j.cemconres.2023.107304

[76] Xu, B., B. Lothenbach, and Z. Li, Properties and hydrates of seawater-mixed magnesium potassium phosphate cements with high magnesium-to-phosphate ratio. Cement and Concrete Composites, 2022. 134: p. 104807. https://doi.org/10.1016/j.cemconcomp.2022.104807

[77] Bernard, E. and H. Nguyen, Magnesium silicate hydrate (M-S-H) stability under carbonation. Cement and Concrete Research, 2024. 178: p. 107459. https://doi.org/10.1016/j.cemconres.2024.107459

[78] Kulik, D., G.D. Miron, and B. Lothenbach, A structurally-consistent CASH+ sublattice solid solution model of fully hydrated C-S-H phases: Thermodynamic basis, methods, and Ca-Si-H2O core sub-model. Cement and Concrete Research, 2022. 151: p. 106585. https://doi.org/10.1016/j.cemconres.2021.106585

[79] Miron, G.D., D. Kulik, Y. Yan, J. Tits, and B. Lothenbach, Extensions of CASH+ thermodynamic solid solution model for the uptake of alkali metals and alkaline earth metals in C-S-H. Cement and Concrete Research, 2022. 152: p. 106667. https://doi.org/10.1016/j.cemconres.2021.106667

[80] Miron, G.D., D.A. Kulik, and B. Lothenbach, Porewater compositions of Portland cement with and without silica fume calculated using the fine-tuned CASH+NK solid solution model. Materials and Structures, 2022. 55(8): p. 212. https://doi.org/10.1617/s11527-022-02045-0

[81] Jo, Y., B. Lothenbach, N. Çevirim-Papaioannou, B. de Blochouse, M. Altmaier, and X. Gaona, Uptake of chloride and isosaccharinic acid by cement paste with high slag content (CEM III/C). Cement and Concrete Research, 2024. 180: p. 107509. https://doi.org/10.1016/j.cemconres.2024.107509

[82] Beaudoin, J.J., V.S. Ramachandran, and R.F. Feldman, Interaction of chloride and C-S-H. Cement and Concrete Research, 1990. 20(6): p. 875-883. https://doi.org/10.1016/0008-8846(90)90049-4

[83] Ma, B. and B. Lothenbach, Thermodynamic study of cement/rock interactions using experimentally generated solubility data of zeolites. Cement and Concrete Research, 2020. 135: p. 106149. https://doi.org/10.1016/j.cemconres.2020.106149

[84] Ma, B. and B. Lothenbach, Synthesis, characterization, and thermodynamic study of selected Na-based zeolites. Cement and Concrete Research, 2020. 135: p. 106111. https://doi.org/10.1016/j.cemconres.2020.106111

[85] Ma, B. and B. Lothenbach, Synthesis, characterization, and thermodynamic study of selected K-based zeolites. Cement and Concrete Research, 2021. 148: p. 106537. https://doi.org/10.1016/j.cemconres.2021.106537

[86] Angst, U., B. Elsener, C.K. Larsen, and Ø. Vennesland, Critical chloride content in reinforced concrete - A review. Cement and Concrete Research, 2009. 39(12): p. 1122-1138. https://doi.org/10.1016/j.cemconres.2009.08.006

[87] Jansen, D., A. German, D. Ectors, and F. Winnefeld, Stacking faults of the hydrous carbonate-containing brucite (HCB) phase in hydrated magnesium carbonate cements. Cement and Concrete Research, 2024. 175: p. 107371. https://doi.org/10.1016/j.cemconres.2023.107371

[88] Rozov, K., U. Berner, D. Kulik, and L.W. Diamond, Solubility and thermodynamic properties of carbonate-bearing hydrotalcite-pyroaurite solid solutions with a 3: 1 Mg/(Al+ Fe) mole ratio. Clays and Clay Minerals, 2011. 59(3): p. 215-232. https://doi.org/10.1346/CCMN.2011.0590301

[89] Collin, M., D.P. Prentice, D. Geddes, J.L. Provis, K. Ellison, M. Balonis, D. Simonetti, and G.N. Sant, Thermochemical data and phase equilibria of halide (Cl−, Br−, I−) containing AFm and hydrotalcite compounds. Journal of the American Ceramic Society, 2024. 107(5): p. 3562-3576. https://doi.org/10.1111/jace.19665

[90] Shi, Z. and B. Lothenbach, The combined effect of potassium, sodium and calcium on the formation of alkali-silica reaction products. Cement and Concrete Research, 2020. 127: p. 105914. https://doi.org/10.1016/j.cemconres.2019.105914

[91] Shi, Z., S. Park, B. Lothenbach, and A. Leemann, Formation of shlykovite and ASR-P1 in concrete under accelerated alkali-silica reaction at 60 and 80 °C. Cement and Concrete Research, 2020. 137: p. 106213. https://doi.org/10.1016/j.cemconres.2020.106213

[92] Maia Neto, F., R. Snellings, and J. Skibsted, Aqueous carbonation of aged blended Portland cement pastes: Impact of the Al/Si ratio on the structure of the alumina-silica gel. Cement and Concrete Research, 2024. 177: p. 107428. https://doi.org/10.1016/j.cemconres.2024.107428

[93] Zajac, M., J. Song, P. Ullrich, J. Skocek, M. Ben Haha, and J. Skibsted, High early pozzolanic reactivity of alumina-silica gel: A study of the hydration of composite cements with carbonated recycled concrete paste. Cement and Concrete Research, 2024. 175: p. 107345. https://doi.org/10.1016/j.cemconres.2023.107345

[94] Wieland, E., G.D. Miron, B. Ma, G. Geng, and B. Lothenbach, Speciation of iron(II/III) at the iron-cement interface: a review. Materials and Structures, 2023. 56(2): p. 31. https://doi.org/10.1617/s11527-023-02115-x

[95] Scrivener, K.L., T. Matschei, F. Georget, P. Juilland, and A.K. Mohamed, Advances in hydration and thermodynamics of cementitious systems. Cement and Concrete Research, 2023. 174: p. 107332. https://doi.org/10.1016/j.cemconres.2023.107332

[96] Bouzouaid, L., A.E.S. Van Driessche, J.C. Martinez, M. Malfois, B. Lothenbach, C. Labbez, and A. Fernandez-Martinez, Impact of gluconate and hexitol additives on the precipitation mechanism and kinetics of CSH. preprint arXiv:2111.02743, 2021.

[97] Dilnesa, B.Z., B. Lothenbach, G. Renaudin, A. Wichser, and D. Kulik, Synthesis and characterization of hydrogarnet Ca3(AlxFe1-x)2(SiO4)y(OH)4(3-y). Cement and Concrete Research, 2014. 59: p. 96-111. https://doi.org/10.1016/j.cemconres.2014.02.001

[98] Dilnesa, B.Z., E. Wieland, B. Lothenbach, R. Dähn, and K. Scrivener, Fe-containing phases in hydrated cements. Cement and Concrete Research, 2014. 58: p. 45-55. https://doi.org/10.1016/j.cemconres.2013.12.012

[99] Pourbaix, M., N. DeZoubov, and J. Van Muylder, Atlas d'Équilibres Électrochimiques. Gauthier-Villars, Paris, 1963.

[100] Lemire, R.J., U. Berner, C. Musikas, D.A. Palmer, P. Taylor, O. Tochiyama, and J. Perrone, Chemical Thermodynamics of Iron - Part 1 - Chemical Thermodynamics. 2013, Nuclear Energy Agency of the OECD (NEA).

[101] Lemire, R., P. Taylor, H. Schlenz, and D. Palmer, Chemical Thermodynamics of Iron - Part 2 - Chemical Thermodynamics. 2020, Nuclear Energy Agency of the OECD (NEA).

[102] Mesmer, R. and C. Baes, The Hydrolysis of Cations. 1976, New York, London, Sydney, Toronto: John Wiley & Sons.

[103] Brown, P.L. and C. Ekberg, Hydrolysis of Metal Ions. 2016: John Wiley & Sons. https://doi.org/10.1002/9783527656189

[104] Hummel, W., U. Berner, E. Curti, F. Pearson, and T. Thoenen, Nagra/PSI chemical thermodynamic data base 01/01. Radiochimica Acta, 2002. 90(9-11): p. 805-813. https://doi.org/10.1524/ract.2002.90.9-11_2002.805

[105] Thoenen, T., W. Hummel, U. Berner, and E. Curti, The PSI/Nagra Chemical Thermodynamic Database 12/07, PSI report 14-04,. 2014, PSI: Villigen, Switzerland.

[106] Grenthe, I., J. Fuger, R.J. Konings, R.J. Lemire, A.B. Muller, C. Nguyen-Trung, and H. Wanner, Chemical Thermodynamics of Uranium. Vol. 1. 1992, Amsterdam: Elsevier.

[107] Furcas, F.E., Reaction pathways of iron in aqueous media. 2024, Eidgenössische Technische Hochschule Zürich.

[108] Schwertmann, U. and R.M. Taylor, Iron Oxides, in Minerals in Soil Environments. 1989. p. 379-438. https://doi.org/10.2136/sssabookser1.2ed.c8

[109] Furcas, F.E., B. Lothenbach, O.B. Isgor, S. Mundra, Z. Zhang, and U.M. Angst, Solubility and speciation of iron in cementitious systems. Cement and Concrete Research, 2022. 151: p. 106620. https://doi.org/10.1016/j.cemconres.2021.106620

[110] Liu, X. and F.J. Millero, The solubility of iron hydroxide in sodium chloride solutions. Geochimica et Cosmochimica Acta, 1999. 63(19-20): p. 3487-3497. https://doi.org/10.1016/S0016-7037(99)00270-7

[111] Frankel, G., Pitting corrosion of metals: a review of the critical factors. Journal of the Electrochemical society, 1998. 145(6): p. 2186. https://doi.org/10.1149/1.1838615

[112] Strehblow, H.H., Breakdown of passivity and localized corrosion: Theoretical concepts and fundamental experimental results. Materials and Corrosion, 1984. 35(10): p. 437-448. https://doi.org/10.1002/maco.19840351002

[113] Wieland, E., G.D. Miron, B. Ma, G. Geng, and B. Lothenbach, Speciation of iron (II/III) at the iron-cement interface: a review. Materials and Structures, 2023. 56(2): p. 31. https://doi.org/10.1617/s11527-023-02115-x

[114] Furcas, F.E., S. Mundra, B. Lothenbach, C.N. Borca, T. Huthwelker, and U.M. Angst, The influence of silicon on the formation and transformation of corrosion products. arXiv:2402.13003 [cond-mat.mtrl-sci], 2024. https://doi.org/10.1016/j.cemconres.2024.107554

[115] Galai, L., L. Marchetti, F. Miserque, P. Frugier, N. Godon, E. Brackx, C. Remazeilles, and P. Refait, Effect of dissolved Si on the corrosion of iron in deaerated and slightly alkaline solutions (pH ≈ 8.1) at 50 °C. Corrosion Science, 2023. 210: p. 110790. https://doi.org/10.1016/j.corsci.2022.110790

[116] Galai, L., L. Marchetti, N. Godon, C. Remazeilles, and P. Refait, Kinetic study of Fe silicates formation during iron corrosion in deaerated and alkaline Si-containing solutions at 50 °C. Corrosion Science, 2023. 211: p. 110846. https://doi.org/10.1016/j.corsci.2022.110846

[117] Albert, C., O.B. Isgor, and U. Angst, A literature-based dataset on pore solution compositions of cementitious systems. 2023: ETH Research Collection.
[118] Furcas, F.E., S. Mundra, F. Somaini, O.B. Isgor, and U.M. Angst, Steel Dissolution in Carbonate Environments. Elsevier Preprint, 2024. https://doi.org/10.2139/ssrn.5044436
[119] Bertolini, L., B. Elsener, P. Pedeferri, E. Redaelli, and R.B. Polder, Corrosion of Steel in Concrete: Prevention, Diagnosis, Repair. 2013: John Wiley & Sons. https://doi.org/10.1002/9783527651696
[120] Angst, U.M., M.R. Geiker, A. Michel, C. Gehlen, H. Wong, O.B. Isgor, B. Elsener, C.M. Hansson, R. Francois, K. Hornbostel, R. Polder, M.C. Alonso, M. Sanchez, M.J. Correia, M. Criado, A. Sagues, and N. Buenfeld, The steel-concrete interface. Materials and Structures, 2017. 50(2). https://doi.org/10.1617/s11527-017-1010-1
[121] Stefanoni, M., Z. Zhang, U.M. Angst, and B. Elsener, The kinetic competition between transport and oxidation of ferrous ions governs precipitation of corrosion products in carbonated concrete. RILEM Technical Letters, 2018. 3: p. 8-16. https://doi.org/10.21809/rilemtechlett.2018.57
[122] Furcas, F.E., B. Lothenbach, S. Mundra, C.N. Borca, C.C. Albert, O.B. Isgor, T. Huthwelker, and U.M. Angst, Transformation of 2-line ferrihydrite to goethite at alkaline pH. Environmental Science & Technology, 2023. 57(42): p. 16097-16108. https://doi.org/10.1021/acs.est.3c05260
[123] Schmid, T., N. Ruffray, M. Griffa, Z. Zhang, O.B. Isgor, and U.M. Angst, Probing the steel-concrete interface microstructure using FIB-SEM nanotomography. Materials and Structures, 2024 (in review). https://doi.org/10.1617/s11527-025-02602-3
[124] Millero, F.J., The effect of ionic interactions on the oxidation of metals in natural waters. Geochimica et Cosmochimica Acta, 1985. 49(2): p. 547-553. https://doi.org/10.1016/0016-7037(85)90046-8
[125] Morgan, B. and O. Lahav, The effect of pH on the kinetics of spontaneous Fe(II) oxidation by O2 in aqueous solution - basic principles and a simple heuristic description. Chemosphere, 2007. 68(11): p. 2080-2084. https://doi.org/10.1016/j.chemosphere.2007.02.015
[126] Stumm, W. and J.J. Morgan, Aquatic Chemistry: Chemical Equilibria and Rates in Natural Waters. 3rd edition ed. 1996, Hoboken, NJ: John Wiley and Sons. 1040.
[127] Pham, A.N. and T.D. Waite, Oxygenation of Fe(II) in natural waters revisited: Kinetic modeling approaches, rate constant estimation and the importance of various reaction pathways. Geochimica et Cosmochimica Acta, 2008. 72(15): p. 3616-3630. https://doi.org/10.1016/j.gca.2008.05.032
[128] Mundra, S., J. Tits, E. Wieland, and U.M. Angst, Aerobic and anaerobic oxidation of ferrous ions in near-neutral solutions. Chemosphere, 2023. 335. https://doi.org/10.1016/j.chemosphere.2023.138955
[129] Furcas, F.E., S. Mundra, B. Lothenbach, and U.M. Angst, Speciation Controls the Kinetics of Iron Hydroxide Precipitation and Transformation at Alkaline pH. Environmental Science & Technology, 2024. 58(44): p. 19851-19860. https://doi.org/10.1021/acs.est.4c06818
[130] Alonso, C., C. Andrade, and J. González, Relation between resistivity and corrosion rate of reinforcements in carbonated mortar made with several cement types. Cement and Concrete Research, 1988. 18(5): p. 687-698. https://doi.org/10.1016/0008-8846(88)90091-9
[131] Stefanoni, M., U.M. Angst, and B. Elsener, Kinetics of electrochemical dissolution of metals in porous media. Nature Materials, 2019. 18(9): p. 942-947. https://doi.org/10.1038/s41563-019-0439-8
[132] Stefanoni, M., U.M. Angst, and B. Elsener, Electrochemistry and capillary condensation theory reveal the mechanism of corrosion in dense porous media. Scientific Reports, 2018. 8(1): p. 7407. https://doi.org/10.1038/s41598-018-25794-x
[133] F. Hunkeler, S.v.G.D., Karbonatisierung von Beton und Korrosionsgeschwindigkeit der Bewehrung im karbonatisierten Beton, in ASTRA/VSS Report 696. 2019: Bundesamt für Strassen, Berne,Switzerland.
[134] Furcas, F.E., A. German, F. Winnefeld, P. Lura, and U. Angst, Durability of MgO/hydromagnesite mortars--Resistance to chlorides and corrosion. arXiv preprint arXiv:2405.08164, 2024.
[135] Wong, H.S., U.M. Angst, M.R. Geiker, O.B. Isgor, B. Elsener, A. Michel, M.C. Alonso, M.J. Correia, J. Pacheco, J. Gulikers, Y. Zhao, M. Criado, M. Raupach, H. Sørensen, R. François, S. Mundra, M. Rasol, and R. Polder, Methods for characterising the steel-concrete interface to enhance understanding of reinforcement corrosion: a critical review by RILEM TC 262-SCI. Materials and Structures, 2022. 55(4). https://doi.org/10.1617/s11527-022-01961-5
[136] Albert, C.C., S. Mundra, D.F. Sanchez, F.E. Furcas, A.D. Rajyaguru, O.B. Isgor, D. Grolimund, and U.M. Angst, Microscale chemical imaging to characterize and quantify corrosion processes at the metal-electrolyte interface. Npj Materials Degradation, 2024. 8(1). https://doi.org/10.1038/s41529-024-00534-x
[137] Pang, Q., H. DorMohammadi, O.B. Isgor, and L. Arnadottir, Density functional theory study on the effect of OH and Cl adsorption on the surface structure of alpha-Fe2O3. Computational and Theoretical Chemistry, 2017. 1100: p. 91-101. https://doi.org/10.1016/j.comptc.2016.12.009
[138] Küter, A., Management of Reinforcement Corrosion a thermodynamic Approach. 2009, Technical University of Denmark.
[139] Küter, A., M.R. Geiker, and P. Møller, On the application of thermodynamics of corrosion for service life design of concrete structures, in 2nd Int. Symp. Service life design for infrastructures. 2010: Delft, Netherlands.